Extremely High Degree of N-Soliton Pulse Compression in an Optical Fiber

Nail N. Akhmediev and Nina V. Mitzkevich

Abstract—**The process of pulse self-compression in an optical fiber is theoretically investigated on the basis of exact N-soliton solutions of the NLS. It is shown that the degree of compression can be approximately N times higher than in the previously considered case of $N/\cosh$-type initial conditions. The evolution of the spectra of N-soliton pulse is also considered.**

I. Introduction

A NUMBER of papers has been presented in the literature which deal with the problem of multisoliton pulse self-compression in an optical fiber [1]–[5]. Mathematically, the problem reduces to following the evolution of the N-soliton solution of the nonlinear Schrodinger (NLS) equation for a given initial condition. If the higher order dispersion, time delay, and other effects are neglected in the fiber, the pulse envelope ψ obeys

$$i\psi_\xi + \tfrac{1}{2}\psi_{\tau\tau} + |\psi|^2\psi = 0 \tag{1}$$

where ξ is a dimensionless longitudinal coordinate, and τ is a dimensionless retarded time variable. The relations between these quantities and physical variables can be found elsewhere [1]–[3]. Since the early work of Satsuma and Yajima [6], the solution of the problem with initial condition

$$\psi = N/\cosh(\tau) \tag{2}$$

has been studied extensively. This is the most simple and convenient form of initial conditions which obeys the exact solution of the NLS in the case of integer N [6]. Equation (2) has also been used for numerical simulations in cases more general than (1) [7], when (2) does not obey the exact solution. But it has been shown [8] that initial condition (2) is not the best one if we wish to obtain the maximum degree of pulse self-compression.

The aim of the present work is to show the existence of initial conditions which lead to both a higher degree of pulse compression and a larger fraction of energy contained in the main peak than the yield of initial condition (2). It is known [6] that the initial condition (2) obeys the exact N-soliton solution with the amplitudes of partial solitons comprising the nonlinear superposition which are equal to half-integers: $1/2$, $3/2$, $5/2$, and so on (N times). It can be shown as well that the phase of each soliton in this superposition is opposite to the phase of the soliton with smaller amplitude, such that the phases of all solitons alternate. However, it is possible to construct a nonlinear superposition of the solitons with the same amplitudes with coincident (for definiteness, equal to zero) phases. In what follows, we shall show that these kinds of solutions are optimal for self-compression. Moreover, for large N, there also exist other phase combinations more profitable for self compression [8] than the case of [6].

For numerical simulation of multisoliton solutions, there exist explicit formulas [9]. However, we have found it more convenient to apply the Darboux transformation [10] in combination with numerical [11] methods for obtaining N-soliton solutions of NLS. We have analyzed these solutions up to $N = 10$ inclusive. The construction of exact solutions enabled us to derive the main relationships governing the process, to determine the dependencies of the compression factor and the energy contained in the main peak of pulse and other characteristics of N-soliton pulses on the value of N, and also to identify the initial conditions under which the process of self-compression proceeds in an optimal manner.

In the optimal case, the maximum amplitude of the compressed pulse is equal to N^2, so that the maximum intensity is N^4. At large N, the degree of self-compression is approximately N times higher than for initial condition (2). The fraction of the energy carried by the main peak of the self-compression pulse relative to the full energy approaches a certain constant $\cong 0.8$, so that the maximum theoretical efficiency of the process is $N^{1/2}$ times higher than in [6]. We have also investigated the appropriate phase chirps for pulses and the evolution of Fourier spectra of the pulse compression process.

II. The Darboux Transformation Formulas and Transformations Diagram

The Darboux transformation formulas for a number of nonlinear equations including the NLS was obtained previously by Sall' [10]. These formulas connect two solutions of NLS (or other nonlinear equation) and eigenfunctions of some set of linear differential equations corresponding to these solutions by algebraic transformations. The eigenfunctions corresponding to one of these solutions should be found solving the eigenvalue problem. Practically, it can be done only for relatively simple solutions of NLS. So, the method allows to obtain more complicate solutions using the simple ones.

It is possible to construct more complex solutions of the NLS successively using the connection between three or more solutions and corresponding eigenfunctions. This connection consists of several stages of Darboux transformation. But it is essential that we can restrict ourselves by solving the eigenvalue problem only once at the lowest level of transformations. All other calculations can be done using solely algebraic transformations. Nevertheless, the full scheme consists of several trans-

Manuscript received May 3, 1990; revised February 22, 1991.

N. N. Akhmediev is with the F. V. Lukin Research and Development Institute of Physical Problems, Zelenograd 103460, Moscow, U.S.S.R., on leave at the Optical Sciences Center, University of Arizona, Tucson, AZ 85721.

N. V. Mitzkevich is with the F. V. Lukin Research and Development Institute of Physical Problems, Zelenograd 103460, Moscow, U.S.S.R.

IEEE Log Number 9144902.

0018-9197/91/0300-0849$01.00 © 1991 IEEE

formations on each stage and requires special diagram of connections between the solutions of the NLS and corresponding eigenfunctions in addition to transformation formulas. Such a diagram was developed and applied in [11] for constructing special "N-modulated" solutions of NLS. But the detailed description of this diagram was not given. We make up for that deficiency in this paper.

For completeness, we briefly review also the basic equations in this section. The Darboux transformation method is based on the ability to represent the NLS for a function $\psi(\xi, \tau)$ in the form of the compatibility condition of the following set of linear equations:

$$R_\tau = UR + lJR,$$
$$R_\xi = (l^2 J + lU + V/2)R \tag{3}$$

where

$$R = \begin{pmatrix} r \\ s \end{pmatrix}, \qquad U = \begin{pmatrix} 0 & i\psi^* \\ i\psi & 0 \end{pmatrix},$$
$$V = \begin{pmatrix} -i|\psi|^2 & \psi_\tau^* \\ -\psi_\tau & i|\psi| \end{pmatrix}, \quad J = \begin{pmatrix} i & 0 \\ 0 & -i \end{pmatrix}. \tag{4}$$

l is a constant (eigenvalue).

For each solution $\psi(\xi, \tau)$ of the NLS, there is a pair of functions r and s (eigenfunction) which depend not only on l, but also on two arbitrary integration constants (we shall call them C and D). A set of these constants together with l will be denoted by $\sigma = \{l, C, D\}$. If we know a certain (seedling) solution of the NLS $\psi = \psi_o(\xi, \tau)$, then in the first stage of the solution process, the functions $r_1(\sigma)$ and $s_1(\sigma)$ can be found only by direct solution of the set of (3). We shall assume that the set of parameters in these functions is fixed so that $\sigma = \sigma_1$. Starting from ψ_o, r_o, and s_o, we can obtain a new solution of the NLS by means of the formula

$$\psi_1(\xi, \tau) = \psi_o(\xi, \tau) + \frac{2(l_1^* - l_1) r_o^* s_o}{|r_o|^2 + |s_o|^2}. \tag{5}$$

The new solution ψ_1 is determined not only by those parameters which influence ψ_o, but also by new parameters σ_1. The power of the numerical methods used in the Darboux transformation approach is that the functions r_1 and s_1 for the next stage, corresponding to the solution of (5), can be found without solving (3) but simply by using an operator M given below and capable of yielding new functions R_1, employing solely algebraic transformations

$$R_1(\sigma_1, \sigma_n) = M[R_o(\sigma_1), R_o(\sigma_n)] \tag{6}$$

where $\sigma_n (n = 2, 3, \cdots, N)$ are other fixed sets of parameters. The number N is the highest order of solution we need in the final stage. The full relationships represented by (6) can be written as follows:

$$\begin{aligned} r_1(\sigma_1, \sigma_n) = \Delta[&(l_1^* - l_1)\, s_o(\sigma_1)\, r_o(\sigma_1)\, s_o(\sigma_n) \\ &+ (l_n - l_1)\, |r_o(\sigma_1)|^2\, r_o(\sigma_n) \\ &+ (l_n - l_1^*)\, |s_o(\sigma_1)|^2\, r_o(\sigma_n)] \\ s_1(\sigma_1, \sigma_n) = \Delta[&(l_1^* - l_1)\, s_o(\sigma_1)\, r_o(\sigma_1)\, r_o(\sigma_n) \\ &+ (l_n - l_1)\, |s_o(\sigma_1)|^2\, s_o(\sigma_n) \\ &+ (l_n - l_1^*)\, |r_o(\sigma_1)|^2\, s_o(\sigma_n)] \end{aligned} \tag{7}$$

where $\Delta = [|r_o(\sigma_1)|^2 + |s_o(\sigma_1)|^2]^{-1}$. Strictly speaking, just these relations between the eigenfunctions R_o and R_1 are called [10] the Darboux transformations. In numerical calculations, the factor Δ does not affect the form of the new solutions of the NLS and it can be dropped.

This process can be continued and new set of $N - \Lambda$ functions $R_\Lambda(\sigma_1, \cdots, \sigma_\Lambda, \sigma_k)$ $(k = \Lambda + 1, \cdots, N)$ depending on $\Lambda + 1$ parameters σ_n are obtained at each stage Λ ($\Lambda = I, II, \cdots, N - 1$). The recurrence formula for this procedure is

$$\begin{aligned} &R_\Lambda(\sigma_1, \cdots, \sigma_\Lambda, \sigma_k) \\ &\quad = M[R_{\Lambda-1}(\sigma_1, \cdots, \sigma_\Lambda), R_{\Lambda-1}(\sigma_2, \cdots, \sigma_{\Lambda-1}, \sigma_k)], \\ &\qquad (k = \Lambda + 1, \cdots, N) \end{aligned} \tag{8}$$

where instead of σ_1 and σ_n in r and s functions in (7) we substitute the sets of parameters $\sigma_1, \cdots, \sigma_\Lambda$ and $\sigma_1, \cdots, \sigma_{\Lambda-1}$, σ_k, respectively. Then, for $\Lambda = I$, (8) reduces to (6).

The new solution of the NLS found at each stage of the calculations can be deduced from the formula

$$\psi_{\Lambda+1}(\xi, \tau) = \psi_\Lambda(\xi, \tau) + \frac{2(l_{\Lambda+1}^* - l_{\Lambda+1}) r_\Lambda^* s_\Lambda}{|r_\Lambda|^2 + |s_\Lambda|^2}. \tag{9}$$

The schematic diagram for constructing of higher order solutions is shown in Fig. 1. The designations in this figure are the same as in the above formulas. The arrows on this diagram show the sequence of actions at constructing the new solutions. A pair of arrows pointing to some vector function $R_\Lambda(\sigma_1, \cdots \sigma_\Lambda, \sigma_k)$ from the bottom denotes the operator M in (8) and defines two vector functions of previous stage $R_{\Lambda-1}(\sigma_1, \cdots \sigma_{\Lambda-1}, \sigma_k)$ used in this operator. A pair of arrows pointing to some solution $\psi_\Lambda(\sigma_1, \cdots \sigma_\Lambda)$ from the bottom denotes (9) and defines the functions used in it for obtaining this solution.

Thus, we first should define the seeding solution ψ_o and the highest order of solution N that we need. Then we should solve the differential equation (3) for obtaining the eigenfunctions $R_o(\sigma)$ corresponding to this solution. Choosing the set of N parameters σ_n, we have the set of N eigenfunctions $R_o(\sigma_n)$. All of them are used in formulas (7) for constructing the set of $N - 1$ eigenfunctions $R_1(\sigma_1, \sigma_n)$ of the second level, but only one $R_o(\sigma_1)$ is used in formula (5) for constructing the first-order solution $\psi_1(\sigma_1)$. This step, as well as all subsequent ones, consists of solely algebraic transformations. The further steps are clear from the diagram.

The selection of the seeding solution ψ_o and of the constants σ_n is determined by the actual physical problem to be solved as well as by the initial and boundary conditions. For example, seeding solution applied to obtain N-soliton solutions is $\psi_o = 0$.

III. Constructing the N-Soliton Solution

To construct N-soliton solutions of the NLS, we shall use the recurrence relations given above. Let us choose as a seeding solution of the NLS the zero solution $\psi_o = 0$. Functions r_o and s_o corresponding to this initial solution have the form

$$r_o = \exp[il_1(\tau - \tau_{01}) + il_1^2(\xi - \xi_{01})]$$
$$s_o = \exp[-il_1(\tau - \tau_{01}) - il_1^2(\xi - \xi_{01})] \tag{10}$$

where l_1, τ_{01}, ξ_{01} are arbitrary parameters of the new soliton solution, to be obtained by (10). The real part of l_1 defines the velocity of a soliton. We shall seek solitons with zero velocity (in our moving frame), so $l_1 = ib_1$ is purely imaginary. The

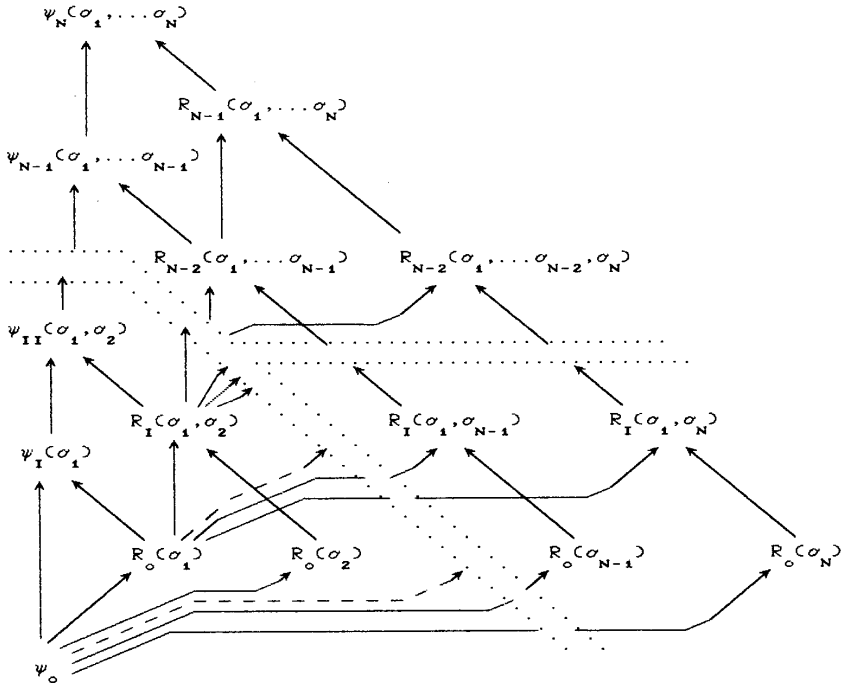

Fig. 1. Darboux transformations diagram for constructing higher order solutions.

real part of l_1 would be responsible for motion of a soliton. In this case, using (6), we obtain a one-soliton solution

$$\psi_I = -\frac{2Ib_1 \exp\,[i2b_1^2(\xi - \xi_{01})]}{ch2b_1(\tau - \tau_{01})} \tag{11}$$

It is convenient to take the parameter b_1 to be equal to 0.5 to obtain the "fundamental soliton" with $N = 1$. On the second step of construction of the two-soliton solution, a new set of parameters b_2, τ_{02}, and ξ_{02} needs to be added. The values b_1 and b_2 have to be unequal for this solution to exist. In our problem of optimal self-compression, the different solitons of the nonlinear superposition must be placed on the same point of the τ-axis. Let us set $\tau_{01} = 0$ and $\tau_{02} = 0$ for definiteness. The two-soliton solution $\psi = \psi_{II}$ can be written in this case in the form

$$\psi_{II} = \frac{4i(b_2^2)\,[b_1 ch(2b_2\tau) - b_2 ch(2b_1\tau)\, e^{i\phi}] \exp\,[i\,2b_1^2(\xi - \xi_{01})]}{(b_2 - b_1)^2\, ch(2b_2\tau + 2b_1\tau) + (b_2 + b_1)^2\, ch(2b_2\tau - 2b_1\tau) - 4b_1b_2 \cos\,\phi} \tag{12}$$

where $\phi = 2b_2^2(\xi - \xi_{02}) - 2b_1^2(\xi - \xi_{01})$, $ch(\tau) = \cosh(\tau)$. If we plug $b_1 = 0.5$, $b_2 = 1.5$, and $\xi_{01} = 2\pi$ in (12), then we obtain the following expression for the two-soliton solution:

$$\psi_{II} = \frac{ch3\tau + 3ch\tau \exp(i4\xi)}{ch4\tau + 4ch2\tau + 3\cos 4\xi} \exp(i\xi/2). \tag{13}$$

This form of two-soliton solution, which is equal to (2) at $\xi = 0$, has been obtained in [6].

Higher Order Solutions

Analytical solutions for multisoliton pulses in cases $N > 2$ are very cumbersome; so we shall construct these solutions only numerically. Exact solutions can easily be constructed up to $N = 10$, but for $N > 5$, calculations need to be done with double precision. The new pair of parameters b_n and ξ_{on} $(1 < n < N)$ should be added in each step of the N-soliton pulse construction. The values $\tau_{on} = 0$ as we mentioned above.

In what follows, we shall point out the restrictions which the parameters b_n can satisfy without loss of generality. 1) Each pair of b_n must be unequal. In the opposite case, we shall not increase the number of solitons in the following step. 2) The negative value of some of the b_n can be changed to positive along with a corresponding simultaneous shifting of the parameter ξ_{on} in such a way that the full solution will not change as a result. Hence, all b_n can be chosen to be positive. 3) Interchanging of some pair of parameters (b_n, b_j) along with a simultaneous interchanging of pair (ξ_{on}, ξ_{oj}) does not change the form of a solution. Therefore, we shall locate all values b_n in increasing sequence $(0 < b_1 < b_2 < \cdots < b_N)$. 4) In principle, all parameters b_n in this sequence are arbitrary. But the consequence of the factorization of all b_n corresponding to a solution $\psi(\xi, \tau)$ by some real number q will be the following elementary transformation of the solution:

$$\psi'(\xi, \tau) = q\psi(q^2, q\tau). \tag{14}$$

Therefore, it is convenient to choose $b_1 = 0.5$ such that the full width of the N-soliton solution coincides with the width of the "fundamental soliton." 5) The choice of the other b_n is defined by the condition of periodicity of the function ψ along the ξ-axis. In order for the period of the N-soliton solution to be equal to

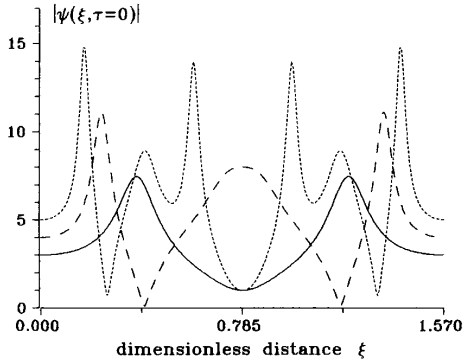

Fig. 2. N-soliton pulse amplitude $|\psi(\xi, \tau)|$ versus ξ at the point $\tau = 0$ for $b_n = (2n - 1)/2$, $N = 3$, $\alpha_n = \{0, 1, 0\}$ (solid curve); $N = 4$, $\alpha_n = \{0, 1, 0, 1\}$ (dashed curve); and $N = 5$, $\alpha_n = \{0, 1, 0, 1, 0\}$ (dotted). These parameters correspond to those in [6].

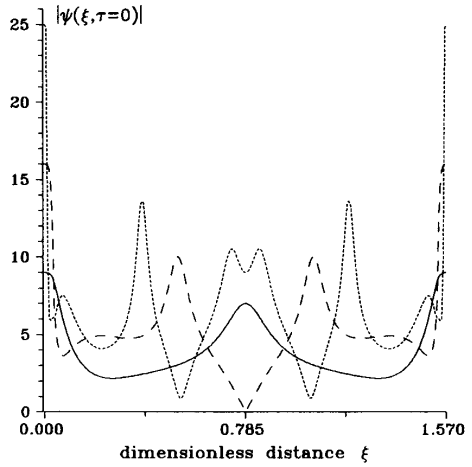

Fig. 3. The same as in Fig. 2 but for zero phases $\alpha_n = 0$.

the period of two-soliton solution (which is equal to $\pi/(b_2^2 - b_1^2)$), all of the b_n's must be half-integers.

The best results from the point of view of self-compression can be achieved for $b_n = (2n - 1)/2$ [8]. Hence, b_n values are the same as in the case considered in [6]. But the relative phases of solitons comprising the pulse should be chosen in a different way. Let us introduce a new variable for the relative phases of each soliton: $\alpha_n = \xi_{on}/2\pi$. In the case of initial condition (2), these values are alternating: $\alpha_n = \{0, 1, 0, 1, 0, \cdots\}$. In this case, the pulse amplitude at the zero point is equal to

$$|\psi(0, 0)| = \left|2 \sum_{n=1}^{N} b_n(-1)^{\alpha_n}\right|. \tag{15}$$

It can be seen from this formula that to achieve a maximal possible amplitude of a pulse at the zero point, it is necessary to set all $\alpha_n = 0$. Thus, we obtain the maximum amplitude of a pulse to be equal to N^2, and the intensity of the pulse at this point is equal to N^4. But we need to find some other initial point on the ξ-axis which correspond to a broad and desirably smooth shape of initial pulse. This choice of initial and final points is in contrast with the case in [6].

The distinction will be clearly seen if we plot the $|\psi(\xi, \tau)|$ dependencies on ξ for $\tau = 0$ and the same N and compare the curves for two cases. These curves describing the envelope behavior in the pulse center upon propagation along the fiber are presented in Fig. 2 (as in [6]) and in Fig. 3 (zero phases case). We choose for simplicity only three values of $N = 3$, 4, and 5. Obviously, the field value in the center of the pulse is maximal in the points ξ_{max} of maximal self-compression. For the same N, these points are not coincided in [6] and in case of zero phases. In [6], initial condition (2) is located at the point $\xi_o = 0$, and the maximum amplitude $|\psi(\xi_{max}, \tau = 0)| \sim N\sqrt{N}$ is achieved at some point ξ_{max}, which is different for different N. In the case of zero phases, the maximum amplitude $|\psi(\xi_{max}, \tau = 0)| \equiv N^2$ takes place in the point $\xi_{max} = 0$ (and at the end of the soliton period $\xi = \pi/2$), but the initial condition should be chosen in some other point ξ_o. This can be done properly using the spectra of pulses. The comparison of envelopes of initial pulses and self-compressed ones in the two cases for $N = 3$ is shown in Fig. 4. The initial and self-compressed pulses for $N = 4$ in the case of zero phases are shown in Fig. 5.

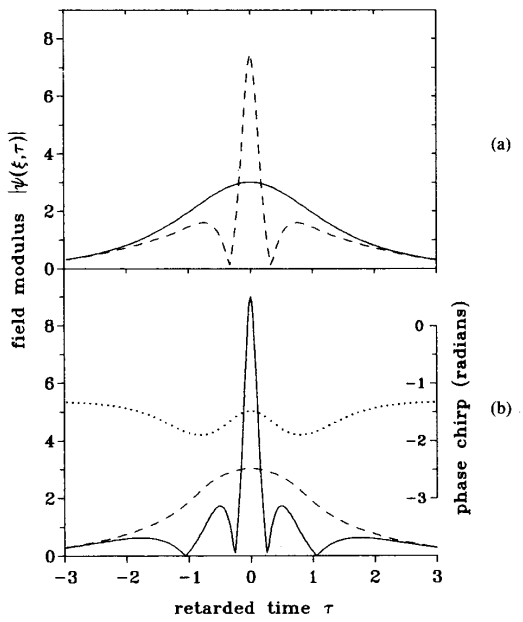

Fig. 4. (a) Envelopes of initial ($\xi = \xi_o = 0$, solid curve) and self-compressed ($\xi = \xi_{max} = 0.372$, dashed curve) pulses for $N = 3$ [6]. (b) Envelopes of initial ($\xi = \xi_o = \pm 0.516$, dashed curve) and self-compressed ($\xi = \xi_{max} = 0$, solid curve) pulses for $N = 3$ zero phase case. The phase chirp of the initial pulse is shown by the dotted curve.

V. Spectral Picture of the Self-Compression Process

The consideration of the self-compression process will be more complete, and the choice of the point ξ_o can be made more conveniently, if we investigate the spectral evolution. The spectrum $f(\omega)$ of a solitary pulse $\psi(\tau)$ can be calculated using the definition

$$f(\omega) = \int_{-\infty}^{\infty} \psi(\tau) \exp(i 2\pi\omega\tau)\, d\tau. \tag{16}$$

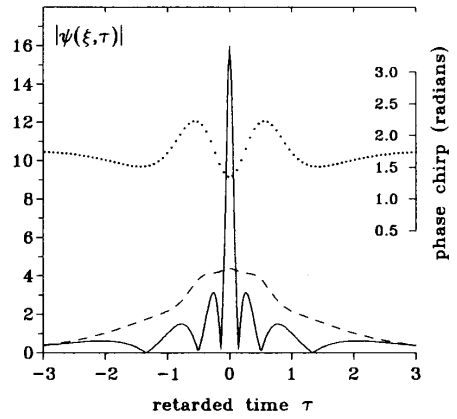

Fig. 5. The same as in Fig. 4(b) for $N = 4$. The value $\xi_o = \pm 0.629$.

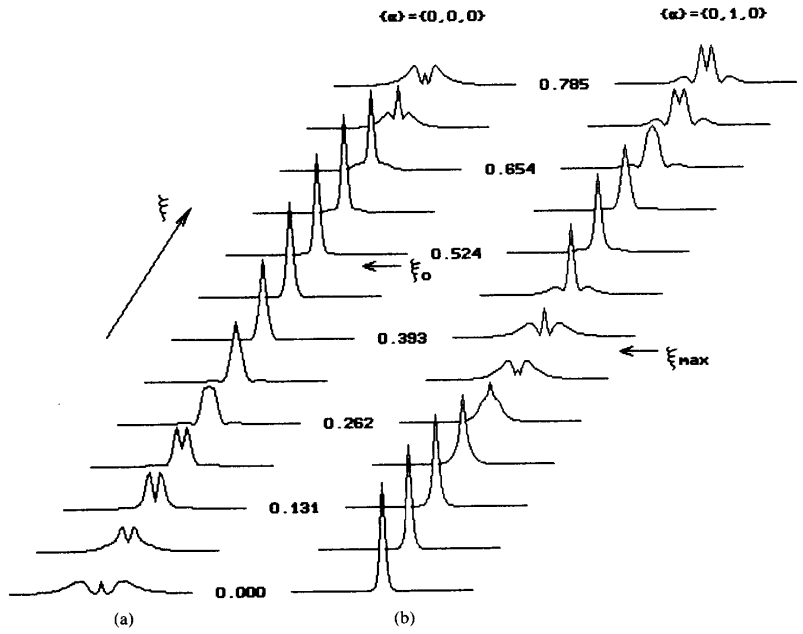

Fig. 6. Evolution of the pulse spectra along the fiber for $N = 3$ for two cases: (a) zero phases; (b) alternating phases. The points ξ_o and ξ_{max} are shown by arrows.

It is more convenient to use in numerical calculations the summation instead of integration (16):

$$f(k\Delta\omega) = \frac{T}{N}\sum_{n=0}^{N-1} \psi\left(\frac{T}{N}n\right) \exp\left(i\,2\pi kn/N\right) \qquad (17)$$

where T is the summation interval on τ, N is the number of points, $\Delta\omega = 1/T$. The functions $f(\omega)$ and $f(k\Delta\omega)$ are approximately coincided in the interval $-(N/2) < k < (N/2)$ for a large number of points N. We calculated the spectra pulses using (17) with the aid of the fast Fourier transform using $N = 256$ or 1024 points.

The examples of spectral evolution for the cases $N = 3$ and $N = 4$ are shown in Figs. 6 and 7, respectively. The cases of spectral evolution for zero phases are shown on the left-hand sides of these figures; the cases of alternating phases are shown on the right-hand sides. It is seen from these figures that for alternating phases, the most narrow spectrum of pulses takes place at $\xi_o = 0$. This spectrum corresponds to the initial condition (2). At the widest point of the spectrum, we should wait for the maximal pulse self-compression. This value of ξ_{max} for the case $N = 3$ is located at 0.372. For the case $N = 4$, this value of ξ is located near the point $\xi_{max} = 0.234$.

For the case of zero phases, the self-compressed pulse with the widest spectrum is located at the point $\xi_{max} = 0$. The narrowest spectrum for the case $N = 3$ takes place near the value of $\xi_o = 0.516$. As can be seen from Fig. 6(a) for $N = 3$, this is the only value ϕ_o inside the soliton half period ($0 < \xi < 0.785 = \pi/4$) at which a narrow spectrum is observed. This

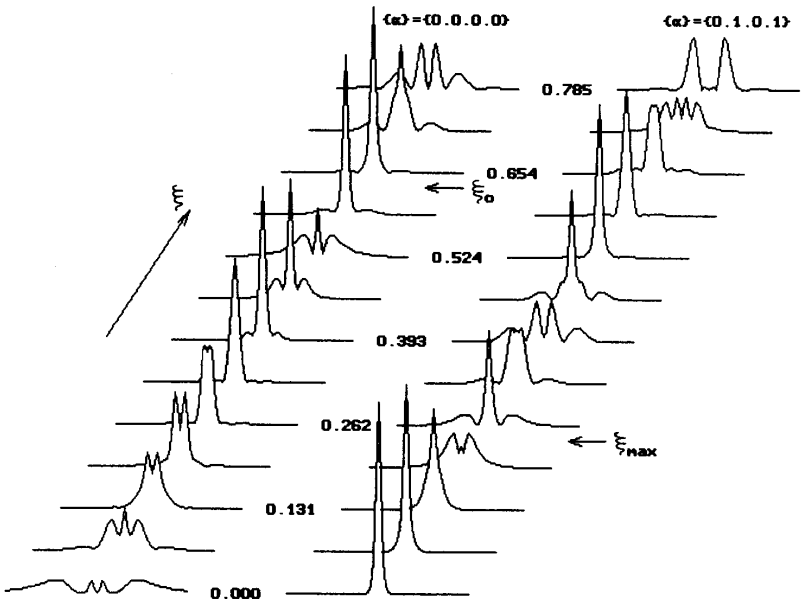

Fig. 7. The same as in Fig. 6 for $N = 4$.

value of ξ_o corresponds to the smooth pulse envelope shown in Fig. 4(b) (dashed curve). For N larger than 3, the choice of ξ_o for initial condition is not single valued. Several possibilities with approximately equal widths of initial pulses exist. The number of these points increases with increasing N. In the case $N = 4$, there are two such values of ξ_o with narrow spectrum: $\xi_o \cong 0.3$ and $\xi_o \cong 0.6$ (see Fig. 7). The smooth pulse envelope takes place near the value $\xi_o \cong 0.63$ (see Fig. 5). The pulse envelope for this value ξ_o is also shown in the inset of Fig. 8 by solid curve. This envelope is compared in this figure to the pulse shape corresponding to the initial condition (2) (dashed curve). The spectra of these two pulses are shown in the upper part of Fig. 8.

The pulse envelope at the point $\xi_o = 0.3$ is not smooth (dotted curve in the inset of Fig. 8). It has approximately the same width as pulse at $\xi = 0.63$, but has three maxima on the top. Nevertheless, this pulse shape and its phase chirp are almost unchanged during propagation from $\xi = 0.2$ up to $\xi = 0.4$. So, the choosing of this initial condition could be more preferable for the self-compression process because of its stability.

There are three values of ξ with narrow spectrum in the case $N = 5$: $\xi_o = 0.31$, $\xi_o = 0.442$, and $\xi_o = 0.626$. The spectra of pulses in the two cases ($\xi_o = 0.442$ and $\xi_o = 0.626$) for $N = 5$ are shown in the lower part of Fig. 8. The spectrum of initial condition (2) is also shown for comparison.

The spectra of self-compressed pulses in two cases (zero phases and [6]) are shown in Fig. 9. The spectrum in the case of zero phases apparently is wider than in [6], and consists of a well-separated central part and sidebands. Sidebands define the main peak of the pulse, and the central part is responsible for the wings.

VI. Self-Compression Parameters

For quantitative evaluation of the pulse self-compression phenomenon, the envelopes of pulses at the moment of maximal compression ($\xi = \xi_{max}$) and at the initial moment ($\xi = \xi_o$) have

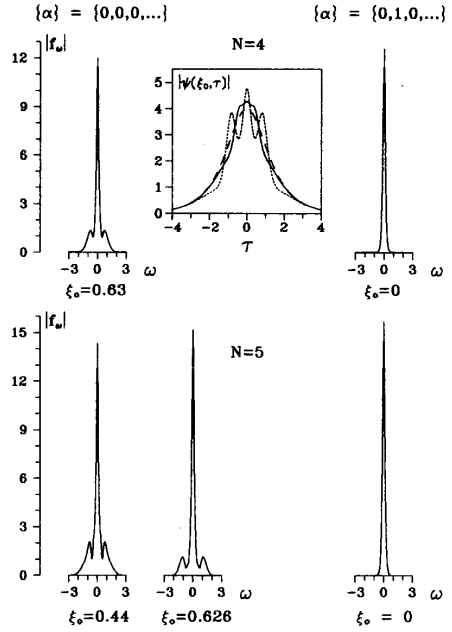

Fig. 8. Spectra of initial pulses for the cases $N = 4$ and $N = 5$ for zero phases (left) and alternating phases (right). Two choices of ξ_o are shown for the $N = 5$ case. The curves in the inset are envelopes of initial pulses for zero phases ($\xi_o = 0.63$—solid curve, $\xi_o = 0.3$—dotted curve) and alternating phases (dashed curve).

to be compared. Let us introduce the following definitions. Let the compression degree Q be the width ($FWHM_{sc}$) of the main peak of the self-compressed pulse divided by the width ($FWHM_{in}$) of the initial pulse

$$Q = FWHM_{sc}/FWHM_{in}. \tag{18}$$

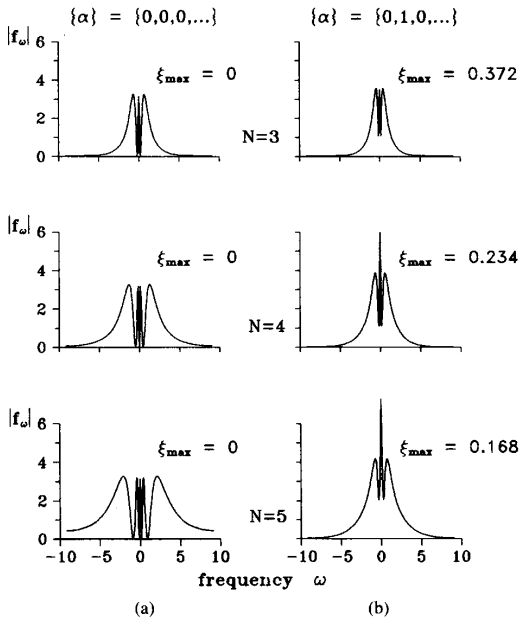

Fig. 9. Comparison of spectra at the point of maximum self-compression for two cases: (a) zero phases; (b) alternating phases for $N = 3, 4, 5$.

Let F be the amplitude of the self-compressed pulse divided by the amplitude of initial one

$$F = |\psi(\xi_{\max}, 0)| / |\psi(\xi_o, 0)|. \tag{19}$$

Let us define the energy coefficient as the ratio of the energy contained in the main peak to the full energy of the initial pulse

$$G = \frac{\int_{-\tau_o}^{\tau_o} |\psi(\xi_{\max}, \tau)|^2 \, d\tau}{\int_{-\infty}^{\infty} |\psi(\xi_o, \tau)|^2 \, d\tau} \tag{20}$$

where τ_o is the zero nearest to the main peak of the pulse envelope.

The dependence of these parameters on the N-value calculated numerically is shown in Figs. 10, 11, and 12, respectively. All of these parameters coincide for $N = 2$ because of coincidence of solutions in this case; but the difference between the two cases increases dramatically with increasing N. We can see from these figures that using zero phases for the solitons is apparently more profitable than alternating phases. It is especially important that, for large N, the majority of the energy of the pulse is concentrated in the main peak, and only 20% of it is continued in the wings. If we wish to avoid the wings completely, we can simply filter the central part of the spectrum because of its separation from that part which is responsible for the main peak. This is clearly seen in Fig. 9(a) for cases $N = 4$ and $N = 5$.

The difference between the considered case and that of [6] is also that the initial field distribution has a phase chirp. The examples of phase distribution across the initial pulse shape are presented in Fig. 4 and 5 for cases $N = 3$ and $N = 4$, respectively. The phase chirp complicates with increasing N. We can avoid this fast dependence and obtain a smooth curve for the phase by choosing another ξ_o. This is illustrated in Fig. 13, where the evolution of the phase is shown along with the evolution of the shape for $N = 3$; but in this case, the curve for the envelope will have a more complicated shape. Both of these cases are equivalent from the point of view of preparation of the initial pulse.

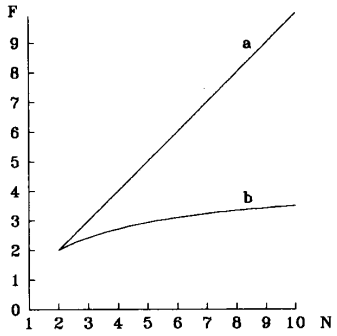

Fig. 10. Maximum amplitude F of the self-compressed pulse relative to the amplitude of initial pulse versus N for two cases: a—zero phases; b—alternating phases.

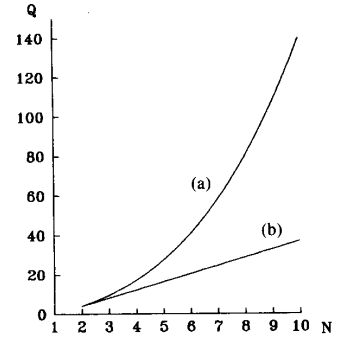

Fig. 11. Self-compression degree Q versus N for two cases: a—zero phases; b—alternating phases.

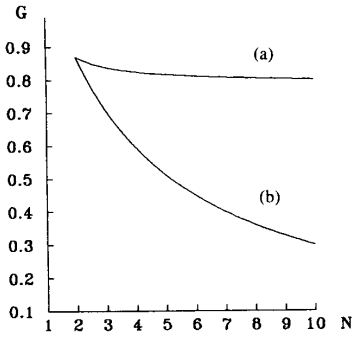

Fig. 12. Energy in the main peak G relative to whole energy versus N for two cases: a—zero phases, b—alternating phases.

VII. Conclusions

The main consequence of this work can be expressed as follows. An N-soliton pulse with zero phases of all constituent solitons is an optimum in the sense that, for a given N, a pulse

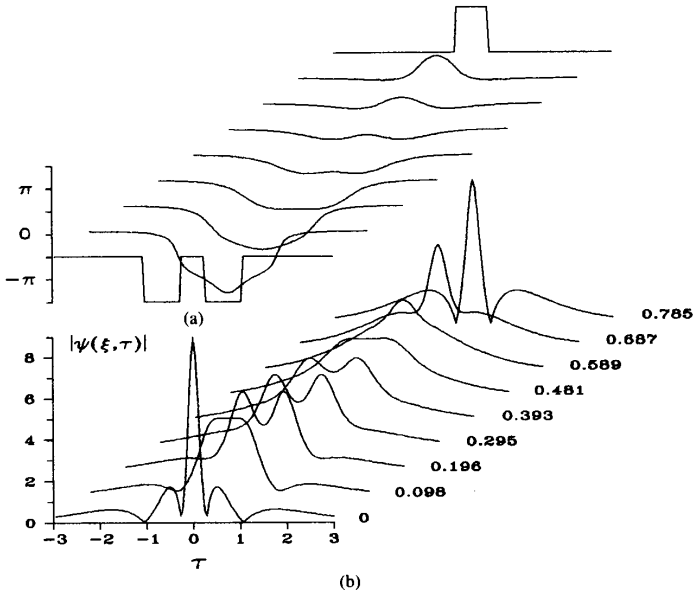

Fig. 13. Evolution of phase chirp (a) and envelope (b) of a pulse in the case of zero phases and $N = 3$. The phase jumps connected with field zeros are equal to π.

can have the maximum possible amplitude N^2 and, hence, the maximum possible intensity N^4 in the center of the evolved pulse. Any other initial conditions which can be investigated numerically (for example, by the beam propagation method) can only approach the above case. This means that the parameters of the self-compression process obtained can serve as a limiting case, because arbitrary initial conditions apart from soliton content have a continuous spectrum (of inverse scattering theory) as well. This is an additional reason for energy loss in the main peak. Even if we suppose that the solitons of the initial pulse have proper amplitudes and zero phases, the presence of continuous spectra will lead to worse self-compression parameters than obtained above. So, the self-compression process considered above in some sense can serve as an ideal one if we limit ourselves to describing the process using the nonlinear Schrodinger equation.

The considered process of pulse self-compression using the special multisoliton pulses might be complicated for experimental realization because of the special initial shape and phase chirp of the pulse required. Nevertheless, this kind of self-compression can be experimentally realized if Wiener and Heritage's technique [12] of pulse preparation is used. Two main difficulties exist in doing this, in our opinion.

First, the solutions found can be unstable relative to small perturbations of initial conditions. This problem can be solved numerically simulating the self-compression process with new initial conditions using the split-step or beam propagation method. Our preliminary investigations show that multisoliton solutions are quite stable for flow values of N such as 3, 4, or 5, but become unstable with increasing N. The proper choice of initial condition is also important. The quantitative estimates of admitted perturbations are required in further investigations.

The second difficulty is concerned with self-induced frequency shift due to Raman effect in a fiber which can separate the solitons in a pulse and destroy the effect of self-compression. Taking this effect into account is also especially important for high values of N. But we can avoid this difficulty by constructing the multisoliton solution with inclusion of this frequency shift into the theory. As a result, we should obtain the initial condition in which the solitons have opposite separations in advance. So, all solitons at the point ξ_{max} of maximal self-compression will be in the same phase, and maximum intensity will be equal to N^4 again. Both problems require special investigations which exceed the limits of this paper.

Acknowledgment

The first author gratefully acknowledges the support of G. I. Stegeman, D. Heatley for valuable discussions and help in writing this paper, and the useful and informative discussions with E. Wright.

References

[1] L. F. Mollenauer, R. H. Stolen, and J. P. Gordon, "Experimental observation of picosecond pulse narrowing and solitons in optical fibers," *Phys. Rev. Lett.*, vol. 45, pp. 1095–1098, 1980.

[2] L. F. Mollenauer and R. H. Stolen, "Solitons in optical fibers," *Fiberopt. Techn.*, no. 4, pp. 193–198, 1982.

[3] L. F. Mollenauer, R. H. Stolen, J. P. Gordon, and W. J. Tomlinson, "Extreme picosecond pulse narrowing by means of soliton effect in single-mode optical fibers," *Opt. Lett.*, vol. 8, pp. 289–291, 1983.

[4] E. M. Dianov, Z. S. Nikonova, A. M. Prokhorov, and V. N. Serkin, "Optimal compression of multisoliton pulses in optical fibers," *Pis'ma Zh. Techn. Fiz., (Sov. Phys.—Tech. Phys.)*, vol. 12, pp. 756–760, 1986.

[5] W. J. Tomlinson, R. H. Stolen, and C. V. Shank, "Compression of optical pulses chirped by self-phase modulation in fibers," *J. Opt. Soc. Amer. B*, vol. 1, pp. 139–149, 1984.

[6] J. Satuma and N. Yajima, "Initial value problems of one-dimensional self-modulation of nonlinear waves in dispersive media," *Progr. Theor. Phys. Suppl.*, no. 55, pp. 284–306, 1974.

[7] G. P. Agrawal, "Effect of intrapulse stimulated Raman scattering on soliton-effect pulse compression in optical fibers," *Opt. Lett.*, vol. 15, no. 4, pp. 224–226, 1990.
[8] N. N. Akhmediev, L. L. Betina, V. M. Eleonskii, N. E. Kulagin, N. V. Ostrovskaja, and E. A. Poltoratskii, "On the optimal self-compression of multisoliton pulses in an optical fiber," *Kvantovaja Elektronika (U.S.S.R.), (Sov. Phys.—Quant. Electron.)*, vol. 16, pp. 1925–1930, 1989.
[9] Z.-Y. Then, N.-N. Huang, and Y. Xiao, "Method for finding soliton solutions of the nonlinear Schrodinger equation," *Phys. Rev. A*, vol. 38, no. 8, pp. 4355–4358, 1988.
[10] M. A. Sall', "Darboux transformations for nonabelian and nonlocal equations of Toda chain type," *Theor. Math. Phys. (U.S.S.R.)*, vol. 53, pp. 227–237, 1982.
[11] N. N. Akhmediev, V. I. Korneev, and N. V. Mitskevich, "*N*-modulation signals in a single-mode optical waveguide under nonlinear conditions," *Sov. Phys.—JETP*, vol. 67, pp. 89–95, 1988.
[12] A. M. Weiner and J. P. Heritage, "Femtosecond pulse shaping and applications," in *Tech. Dig., IQEC'88*, Tokyo, Japan, July 1988, pp. 690–691, Paper ThH-4.

Nail N. Akhmediev, photograph and biography not available at the time of publication.

Nina V. Mitzkevich, photograph and biography not available at the time of publication.